Journal of Engineering and Computer Sciences
Vol. 17, No. 1, pp.56-68 (Jan 2025)

Lateral Torsional Buckling of FRP Beams; Effect of Fiber Orientation and Stacking Sequence

Saleh M. Alogla*
Department of Civil Engineering, College of Engineering, Qassim University, 51452 Buraydah, Qassim, Saudi Arabia.
E: sa.alogla@qu.edu.sa

[Received: 12 June 2024, Revised: 14 August 2024, Accepted: 30 August 2024, Published Jan 2026]

Abstract: This study investigates the influence of fiber orientation and stacking sequence on the lateral-torsional buckling (LTB) behavior of FRP I-beams. The assessment of LTB capacity of beams was conducted using a validated 3D numerical model that allows for varying the stacking sequence and fiber orientation. Several stacking sequences are examined by varying the angles of the fibers. Beams with unidirectional fiber laminates exhibited optimal LTB resistance when the flange fibers aligned with the longitudinal axis (0°) and the web fibers inclined at 45°. Deviations from these angles led to a substantial reduction in LTB capacity. Stacking sequences incorporating a combination of cross-ply and angle-ply layers demonstrated superior LTB performance compared to purely angle-ply configurations. The study further explores the impact of fiber orientation on the required flange thickness to achieve a specific LTB load. Results indicate that lower inclination angles in the flanges allow for thinner flange designs. These findings emphasize the importance of optimizing fiber orientation and stacking sequence during the design of FRP beams to maximize their LTB resistance and achieve efficient load-carrying capacity.

Keywords*:* Lateral torsional buckling, fiber reinforced polymer, fiber orientation, stacking sequence.

1. INTRODUCTION

Fiber-reinforced polymer (FRP) beams have gained significant consideration in structural engineering applications over the past few decades due to their advantageous properties. These superior properties include a high strength-to-weight ratio, improved durability compared to traditional materials, and cost-efficiency in specific applications. However, their relatively low stiffness compared to strength raises concerns about their stability under bending loads (Davalos and Qiao, 1997). One of the main stability concerns in FRP beams subjected to in-plane moment gradients is that the beam at a particular level of loading may fail by deforming laterally and twisting simultaneously (Ascione et al., 2013; Davalos and Qiao, 1997; Karthick et al., 2023; Liu, 2017; Qiao et al., 2002; Singh and Chawla, 2019). This phenomenon is known as lateral-torsional buckling (LTB) or flexural-torsional buckling, and it is more susceptible in FRP beams since bending-twisting coupling exists in many configurations of composite laminates.

When a wide flange (WF) I-beam is subjected to bending, deflection starts to occur as the applied loading increases. At a certain point of increasing the load, an abrupt out-of-plane deflection occurs coupled with twisting of the cross-section of the beam as shown in Figure 1. The sudden loss of stability, observed at the load point on the load-lateral deflection curve, is known as the bifurcation load. At this load, the beam is deemed to have buckled laterally, owing to the effects of LTB. This type of beam instability might develop while the beam's material still behaves elastically or after the cross-section material has partly or fully transformed to the plastic range of the stress-strain curve. In this presented study only the elastic lateral torsional buckling is considered since the behavior of fiber-reinforced polymer, FRP I-beams are assumed to follow Hooke's law of elasticity.

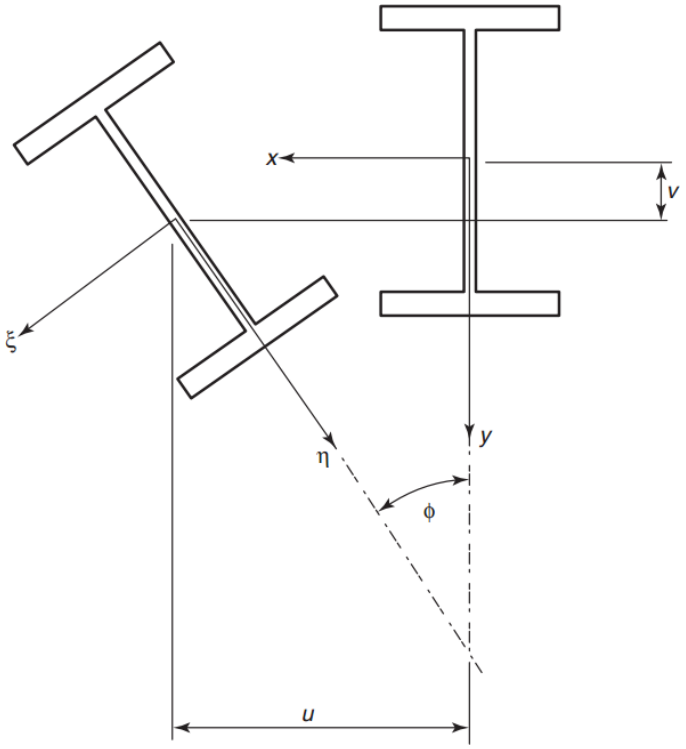

Fig. 1: Schematic of I-beam section before and after lateral-torsional buckling (adopted from (Galambos and Surovek, 2008))

Lateral torsional buckling commonly occurs at the maximum moment cross-section at mid-span for a simply supported I-beam with a concentrated load at mid-span.Several researchers have proposed analytical and numerical solutions for this problem since Timoshenko and Gere (1961) ((Timoshenko and Gere, 2012)) first presented their closed-form solution based on solving the governing differential equations of the problem for a beam made of homogenous isotropic material. Analytical solutions based on the strain-energy method for predicting the lateral-torsional buckling load for the case of FRP WF I-beams are also proposed by a few researchers. Davalos et al. (Davalos and Qiao, 1997) presented an analytical and experimental study on lateral-torsional and lateral-distortional buckling of WF FRP I-beams. Sapkas and Kollar (Sapkás and Kollár, 2002) solved the critical moment of lateral-torsional buckling for various boundary conditions and load cases and presented a closed-form solution for predicting the critical moment taking into account transverse shear and restrained warping-induced shear deformations. In general, deriving closed-form solutions for LTB problems is tedious and impossible in some cases. This led to an increase in numerical evaluation studies supported by validation against experimental results. Further, the possibility of other types of buckling in FRP beams diverted the efforts in research studies to cover the problem.

In general, buckling failure of FRP beams can include localized buckling within the material itself, global buckling due to lateral bending, twisting, or bending in a large-scale way, and even buckling caused by the combination of local and global instabilities. Research has dedicated significant effort to understanding how local buckling affects FRP beams with various shapes (profiles) across their cross-sections (Correia et al., 2011; Estep, 2014; Liu and Harries, 2018). These investigations have utilized a variety of methods, including experimental tests (Ganesan and Kumaran, 2018; E. D. S. Vieira et al., 2018; J. D. Vieira et al., 2018) and analytical or simulation techniques (Ascione et al., 2013; Silva et al., 2011). Similarly, global buckling has been extensively studied, with research examining buckling due to bending, twisting, and lateral forces individually or combined. Literature research has covered various beam section types, including I-beams, angled sections, rectangles, channels, and strips.

Limited studies, however, have investigated the factors influencing the LTB phenomenon in FRP composite beams. Mottram (1992) employed a combined experimental and numerical approach to validate theoretical predictions for LTB in pultruded I-beams (Mottram, 1992). The study validated theoretical predictions for LTB in pultruded I-beams through experiments, employing a finite difference method and thin-walled theory. It also demonstrated the adaptability of classical isotropic theories to predict buckling loads in orthotropic composite beams. Mottram's early investigations affirmed the conservatism of the capacity predictions based on the American design manual under certain testing conditions (i.e. Mid-span point load at the centroid of the I-section beams). Barbero and Raftoyiannis (Barbero and Raftoyiannis, 1994) studied lateral and torsional buckling of composite FRP I-beams using plate theory and including bending-twisting coupling effects. Pandy et al. (1995) examined the effect of fiber orientation of pultruded I-beams by using the Galerkin method to solve the equilibrium differential equations. The study concluded on optimum angles for both web and flanges (Pandey et al., 1995). This study revealed that deviating from the unidirectional fiber orientation inherent to the pultrusion process by introducing an angle in the web fibers can, in certain cases, significantly enhance the buckling load capacity.

Thumrongvut and Seangatith (2011) investigated the lateral-torsional buckling behavior of pultruded FRP channel beams under cantilever loading based on experimental tests on 26 specimens with varying unbraced lengths. The results revealed two response categories based on linear elastic behavior and showed that the modified LFRD steel design equation accurately predicts critical buckling moments for slender beams but overestimates them for shorter beams (Thumrongvut and Seangatith, 2011). Liu et al. (2019) examined the combined effects of lateral-torsional buckling (LTB) and local section distortion (LSD) on the flexural capacity of pultruded GFRP I-sections (Liu et al., 2019). An analytical model using the energy method is proposed to predict critical LTB moments, considering the influence of LSD. The model is validated through experiments and finite element analysis, demonstrating its accuracy for both LTB-dominated and LSD-influenced sections. This approach provides a more refined prediction tool for GFRP I-beam design. Halim (2020) presents closed-form analytical solutions for the critical buckling load of thin-walled, anisotropic composite cantilever beams (rectangular and I-shaped) subjected to pure bending (Halim, 2020). The solutions are validated through finite element analysis and existing theory, demonstrating their accuracy for various composite beam configurations.

Previous researches on LTB revealed that several factors can influence the critical LTB load of FRP beams, including boundary conditions, loading type, cross-sectional geometry, slenderness ratio, and fiber orientation within the laminate plies (Baylor, 2021; Zeinali et al., 2024). For instance, for a simply supported beam subjected to a concentrated load at mid-span, the position of a concentrated load along the cross-section can significantly affect the LTB load. Similarly, contribution of other factors to LTB, such as fiber orientation and stacking sequence, have not fully addressed in literature. Limited research has investigated the influence of fiber orientation and laminate stacking sequence on the capacity of FRP beams under lateral-torsional buckling (LTB). This study addresses this knowledge gap by employing a 3D numerical model to identify optimal design angles for flange and web laminates in FRP I-beams and the differences between various stacking sequences. After validating the model against existing tests in the literature, the model is utilized to quantify the differential LTB load offered by various laminate configurations. The findings aim to serve as a reference, highlighting the importance of considering fiber orientation and stacking sequence in optimizing the LTB performance of FRP beams.

2. NUMERICAL MODEL FOR LATERAL TORSIONAL BUCKLING

A 3D finite element model is developed using ABAQUS (ABAQUS, Dassault Systèmes, 2014) finite element software to assess the influence of fiber orientation and stacking on the LTB of FRP I-beams. The problem conditions were selected as simply supported beam with a concentrated load at mid-span. The model's main purpose is to predict the critical load at which lateral torsional buckling occur.

3. MODEL PROPERTIES

The model is constructed to match existing two large-scale I-beams experiments (Davalos and Qiao, 1997). The simply supported beam built in the model has a cross section with a flange width and web depth of 12 inches (304.8 mm) and a span of 14.5 feet (4.42 m). The thickness of both the flange and the web is ½ inch (12.7 mm). Since the beams in experiments are stiffened with a wooden stiffener at the mid-span cross-section, the model includes a stiffener at mid-span as shown in Figure 2. The I-beam cross-section is composed of laminates for each of the two flanges and the web in which a perfect bond exists between the top and bottom flanges and the web.

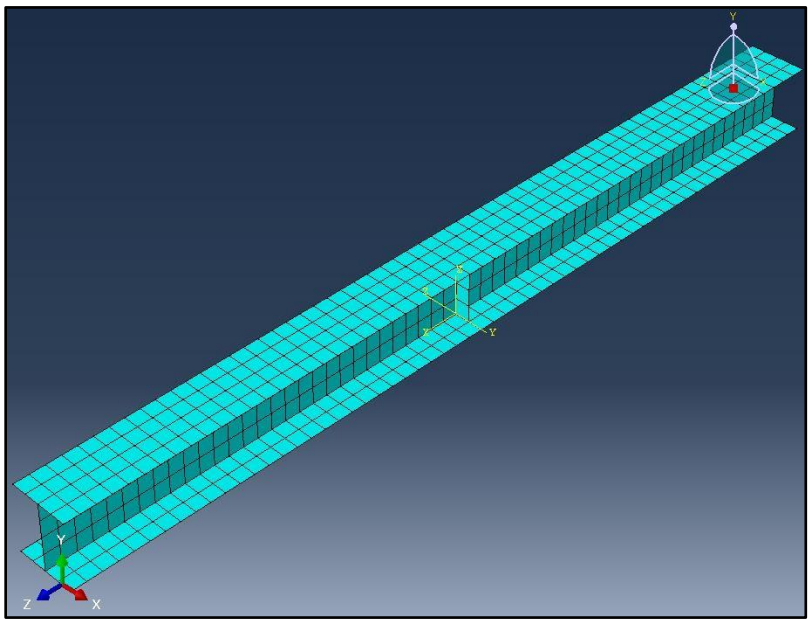

Fig. 2: Constructed 3D model for predicting the critical LTB load for FRP I-beams

The type of element selected for analysis of FRP beams in the developed model is SC8R continuum shell element from ABAQUS library (ABAQUS, Dassault Systèmes, 2014). The utilized mesh size is 3 inches (76mm) for the whole model which yields 4 elements along the flange and 58 elements along the length of the beam. This mesh size is selected to match and compare the model results with those of the finite model developed by Davalos et al. (Davalos and Qiao, 1997) using ANSYS. The wood stiffener at mid-span is modeled by 2 elements along its width and four elements along its depth. Transverse shear through the laminate is considered in the ABAQUS model with one-point integration.

Material properties are assumed based on beams manufactured with glass fibers, and a polyester resin as shown in Table 1 (P. Sodan et al., 1998). Three materials are utilized in the model: GFRP laminates, continuous strand mats (CSM), and wood. The model allows for selecting the layers of laminates and direction of fibers for both flange and web. This is utilized to study three different types of stacking sequence of laminates in FRP I-beams. The angles of fiber orientations in both flange and web can be varied in the model from 0 to 90° allowing to perform a parametric analysis on the effect of fiber orientation on the LTB critical load.

Table 1 Assumed material properties for ABAQUS model

Material	Assumedbehavior	Densitylb/in^3	E11 (ksi)	E22 (ksi)	Poisson's ratio ν12	G12 (ksi)	G23 (ksi)	G13 (ksi)
GFRP	Lamina	0.065	7000	2500	0.28	840	840	840
Wood	Isotropic	0.0174	1400	-	-	-	-	-
CSM	Isotropic	0.11×10^{-4}	1160	-	-	-	-	-

4. MODEL VALIDATION

The model is validated by simulating two experimental results presented by Davalos et al. (Davalos and Qiao, 1997) for pultruded simply-supported FRP I-beams subjected to a concentrated load at mid-span. The two beams (B1 and B2) have stacking sequences consisting of continuous strand mats (CSM), and rovings of +/-45 stitched fabrics (SF) as shown in Figure 3. The implemented stacking sequences for beams 1 and 2 are $[CSM/\pm45]_7$ and $[CSM/0/90)_2/(CSM/\pm45)_3/(CSM/0/90)_2]$, respectively. The cross section of B1 and B2 is identical in dimensions with a flange width and web depth of 12 inches (304.8 mm) and a span of 14.5 feet (4.42 m). The thickness of both the flange and the web is ½ inch (12.7 mm) (Figure 3). Both beams are stiffened with a wooden stiffener at the mid-span cross-section. A unit concentrated load is applied at the middle of the top flange for analysis.

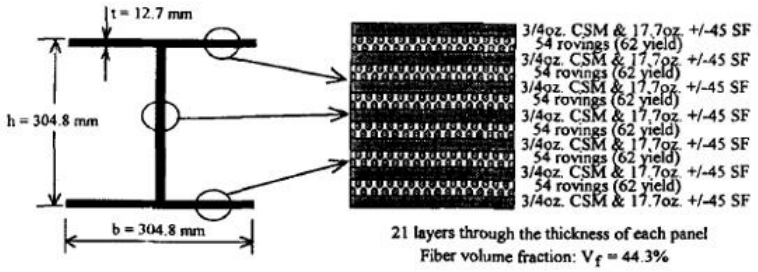

3-a) Beam 1 (B1) cross-section dimensions and stacking sequence

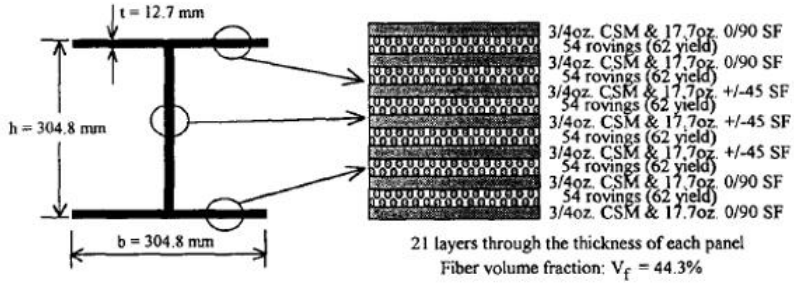

3-b) Beam 2 (B2) cross-section dimensions and stacking sequence

Fig. 3: Adopted beams for validation of the developed ABAQUS model (Davalos and Qiao, 1997).

Eigenvalue analyses were performed for the two reported experimental cases and bifurcation lateral-torsional buckling load were compared with the reported finite element model and experimental results of Davalos et al. (Davalos and Qiao, 1997) in Table 2. The comparison shows an acceptable agreement between the two finite element models prediction for critical buckling load. Both the numerical model presented in this study and Davalos's model underestimate the buckling load based on the experimental results. The developed model underestimates the critical load for B1 with an error of around 20% for B1 and 13% for B2. Similarly, Davalos et al. (Davalos and Qiao, 1997) finite element model showed an error of 26.36% and 26.66% for beam 1 and 2 respectively. This error can be partially attributed to the fact that the tested beams had reduced unbraced length due to the configuration of the end supports (Davalos and Qiao, 1997). Figure 3 shows the meshed beam and the lateral torsional buckling mode for the two analyzed cross sections of beams 1 and 2.

Table 2 Validation of the developed model with Davalos's numerical and experimental results

Beam No.	**MODEL P_{cr}** (kips)	**Davalos's MODEL P_{cr}** (kips)	**Experiments P_{cr}** (kips)
B1	24.56	22.88	31.07
B2	27.27	22.97	31.32

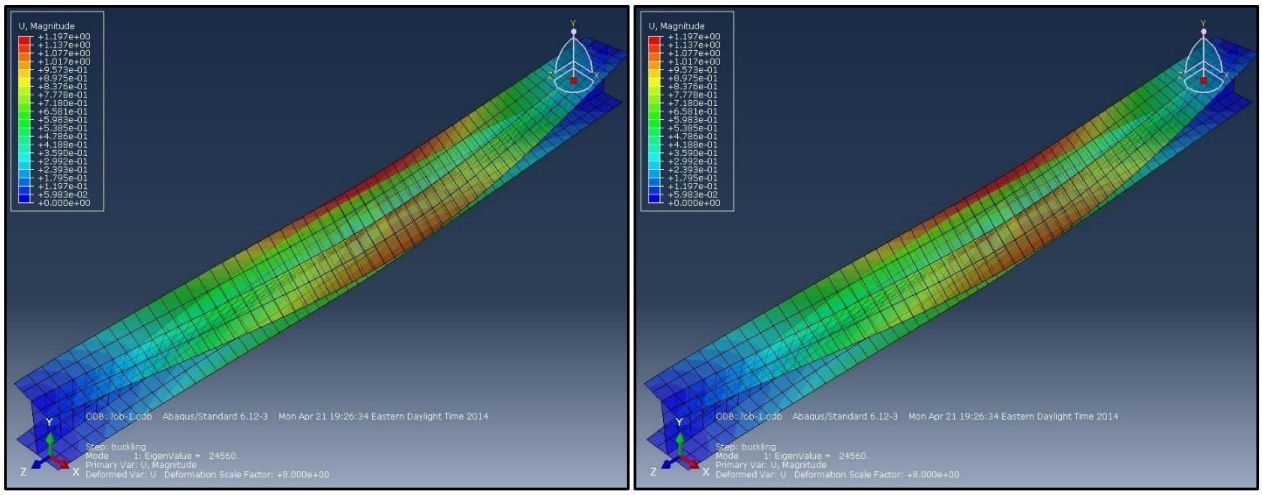

3-a) B1 buckling mode shape

3-b) B1 buckling mode shape

Fig. 4: Shape of I-beam buckling modes as predicted by model for the two beams

5. MODEL VALIDATION

The finite element model developed using ABAQUS is then utilized to perform parametric studies on the lateral-torsional buckling load of the same tested beams cross sections with varying fiber orientation angles and stacking sequences. Several three laminate types are investigated in this study to be used for both the flanges and the web. All three studied laminates are composed of unidirectional fibers. For the flange laminates the angle θ is the rotation of the fiber with respect to the axis along the beam longitudinal axis z in the x-z plane (flange plane-Figure 2). For the web laminates the angle θ represents rotation with respect to the longitudinal axis z in the z-y plane (web plane). In addition to these three cases, an additional case was analyzed in which the required thickness for the flange is assessed based on a fixed critical buckling load and with varying the angle of fibers.

- **Case 1**

The first laminate is constructed with an angle-ply stacking sequence with continuous strand mats, CSM, in between each pair of angle-ply layers, as $[CSM/\ \pm\theta]_7$. For the first laminate stacking sequence of wide flange I-beam cross section of $[CSM/\ \pm\theta]_7$, the variation of the unidirectional fiber is studied by varying θ in the flange laminates and fixing θ to be equal to 45° in the web laminate. Then, the angle θ is varied in the web laminate and kept constant to 45° for the flange laminates.

- **Case 2**

The second laminate is constructed using a combination of cross-ply, CSM, and angle-ply configuration as $[(CSM/0/90)_2/(CSM/\pm\theta)_3/\ (CSM/0/90)_2]$. Similarly for the second case of laminate stacking sequence of $[(CSM/0/90)_2/(CSM/\pm\theta)_3/(CSM/0/90)_2]$, the web angle is fixed to be constant with value of 45° while the flanges angle is varied. Then the flanges angle is fixed to a value of 45° and the web angle is varied.

- **Case 3**

The third laminate type investigated in this parametric analysis is constructed of quasi-isotropic laminate and CSM between each two layers. A quasi-isotropic laminate is made by layering individual plies in a specific way to achieve similar strength and stiffness in all in-plane directions. For this case of quasi-isotropic laminates, a number of five angles are selected to study the behavior of such laminates (15°, 30°, 45°, 60°, and 90°). The stacking sequence depends on the angle between each two plies since the number of plies is related to the constant angle between them ($\theta=\pi/n$), where n represents the number of plies. For instance, an angle of θ=45° between plies yield several 4 plies and CSM between each two plies in the model. Thus, 6 plies are used for the full thickness of ½ inch of the flange.

- **Case 4**

This study employed the critical lateral-torsional buckling load of [CSM/±θ]7 laminates in both web and flanges to assess the impact of flange fiber orientation on the required flange thickness for resisting LTB load. The critical LTB load can be achieved for [CSM/±θ]7 flange laminates with varying angles (30° to 75°) by adjusting the flange thickness. This adjustment, however, necessitates an increase in the total number of plies required. This is critical in highlighting the reduction in flange thickness that can be achieved based on selected fiber orientation.

6. RESULTS AND DISCUSSION

The analysis results on the different laminate cases show a significant variation in critical buckling load due to the change in fiber orientation angles for each stacking sequence case. For the first case of parametric studies, Case 1 ($[CSM/\ \pm\theta]_7$), the results of varying θ for the flanges while fixing the angle of web, and results of varying angle of web while flange is fixed are shown in Figure 5. The results of the critical load are normalized based on the maximum buckling load, $P_{cr,max}$. As demonstrated by the plotted results, it can be inferred that the optimum angle for the flange fibers is 0° along the longitudinal axis of the beam. Similarly, for the web fiber orientation angle, the ideal angle for fiber orientation is 45°. These angles yielded the highest critical buckling loads.

The results show that the change of fiber orientation in flanges influences the resistance to LTB significantly. When the angle in fiber orientation exceeds 30° along the longitudinal axis of the beam, a reduction in LTB capacity of more than 20% occurs. At degrees of 45° to 90°, the LTB capacity of the beam drops significantly to reach only about 60% of the maximum capacity at 0° fiber orientation.

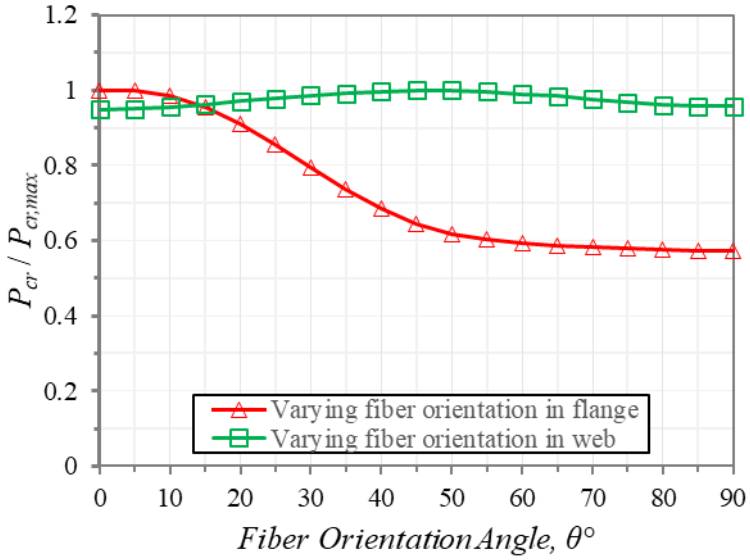

Fig. 5: Fiber orientation effect on LTB load for $[CSM/\pm\theta]_7$ laminate (Case 1)

For Case 2, the results of varying θ for the flanges while fixing the angle of the web, and results of varying the angle of the web while the flange's fiber orientation is fixed are shown in Figure 6. The results of the critical load are normalized based on the maximum buckling load, $P_{cr,max}$. As revealed by the results, the optimum angle for the flange fibers is 0° along the longitudinal axis of the beam as was in case 1. Similarly, for the web fiber orientation angle, the ideal angle for fiber orientation is 45°. However, the results of the different stacking sequences in Case 2 showed a lower reduction in the LTB capacity of I-beams compared to Case 1. When the angle in fiber orientation exceeds 45° along the longitudinal axis of the beam, a reduction in LTB capacity of only around 20% follows (40% in Case 1) (Figure 6).

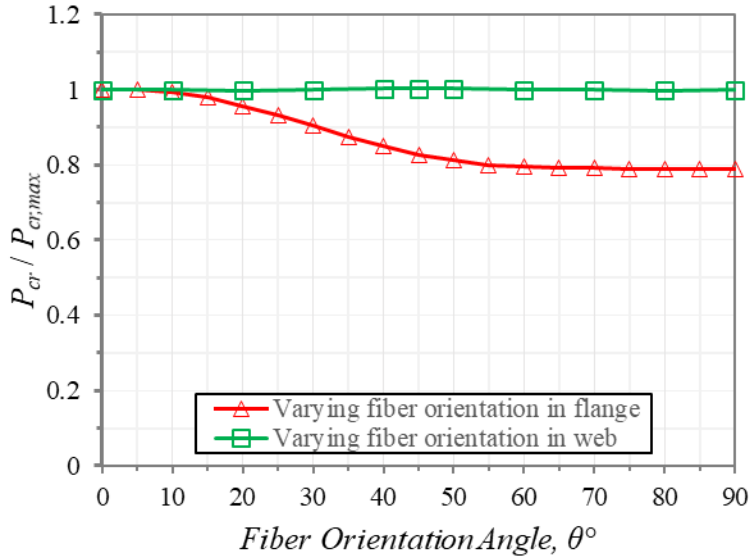

Fig. 6: Fiber orientation effect on LTB load for $[CSM/0/90)_2/(CSM/\pm\theta)_3/(CSM/0/90)_2]$ laminate (Case 2)

For Case 3, quasi-isotropic laminate, the angles selected for fiber orientations are 5 angles ranging from 15° to 90°. As the angle is reduced between the plies, the number of plies increases for a quasi-isotropic laminate. This led to predicting a maximum LTB load at an angle of 15°. The angles of 30° and 45° yielded similar LTB capacity, while the lowest value at an angle of 90°.

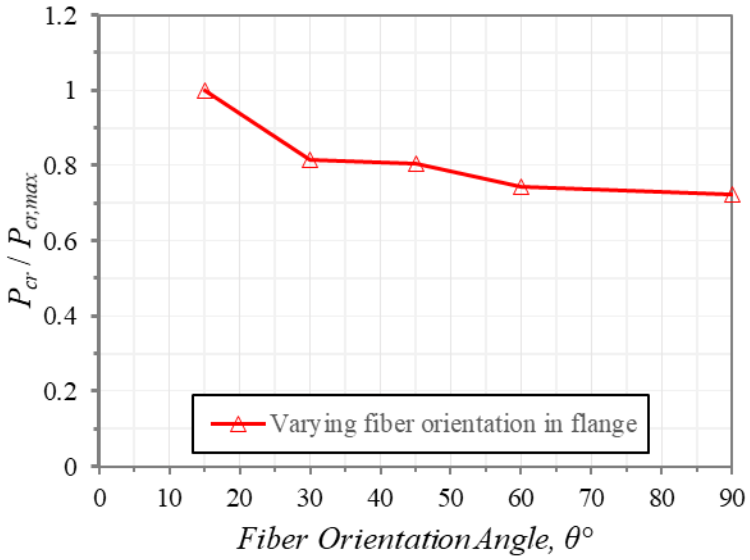

Fig. 7: Fiber orientation effect on LTB load for quasi-isotropic and CSM (Case 3)

For Case 4, Figure 7 shows the required flange thickness to yield a bifurcation lateral torsional load of 24.5 kips for $[CSM/\pm\theta]_7$ at four different angles (30°, 45°, 60°, 75°). As can be interpreted from the numerical generated results, the required thickness to resist the fixed load increases as the angle of the fibers increases. When the angle of fibers is changed from 30° to 75°, an increase of about 37.5% in thickness is required to resist the same load.

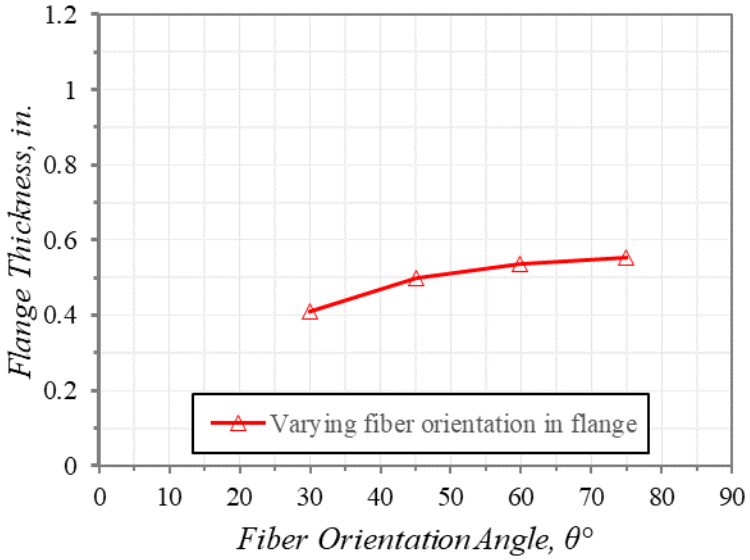

Fig. 8: Effect of fiber orientation on minimum flange thickness for a given load (24.5kips) (Case 4)

7. CONCLUSION

The influence of fiber orientation and stacking sequence on the lateral-torsional buckling (LTB) behavior of wide-flange FRP I-beams has been examined in this study. A validated numerical model developed in ABAQUS was employed to analyze a simply supported FRP beam subjected to a mid-span concentrated load. Three laminate stacking sequences were evaluated in the analysis. The results of the study highlight the importance of considering fiber orientation and stacking sequence for optimal LTB resistance in FRP beam design. The following conclusions can be drawn from the results:

- For beams laminates of CSM (Case 1), the optimum angles for fibers are 0° and 45° for the flange and web respectively. When fiber orientation in the flanges deviates from the beam longitudinal axis the lateral-torsional buckling load reduces up to about half its maximum value (beyond 45°). For the web, however, fiber orientation showed less effect than the flanges with a maximum reduction in lateral-torsional buckling load of about 8%.
- For variant stacking sequence (Case 2) $[(CSM/0/90)_2/(CSM/\pm\theta)_3/(CSM/0/90)_2]$, similar behavior to the CSM case is generated. However, a lower reduction in LTB load is estimated since fewer varied orientation plies are used in the flanges and web (compared to Case 1). Thus, the number of plies varied in fiber orientation controls the magnitude of the LTB load estimated.
- For the case of quasi-isotropic laminates both the angle between the plies and the numberof plies is varied in the four studied angles. As the angle between the plies increases and the number of layers decreases for a constant laminate thickness, the LTB load decreases.
- For beams with CSM laminates, a constant LTB (lateral-torsional buckling) load was used to determine the required flange thickness by varying the fiber orientation angle (θ). Lower inclination angles (θ) of the fibers relative to the beam's longitudinal axis resulted in a thinner flange requirement.
- For FRP I-beams constructed with unidirectional fiber laminates, the fiber orientation in the plane of the beam's longitudinal axis shows remarkable effect on the lateral-torsional buckling load and should be considered in analysis and design. Moreover, the behavior of different laminate stacking sequences shows that higher loads can be resisted before buckling for beams with laminate that utilizes hybrid stacking sequence of cross-ply and angle-ply layers.

REFERENCES

1. ABAQUS, Dassault Systèmes, 2014. ABAQUS Documentation, 6.14. ed. Providence, RI.
2. Ascione, L., Berardi, V.P., Giordano, A., Spadea, S., 2013. Buckling failure modes of FRP thin-walled beams. Composites Part B: Engineering 47, 357–364. https://doi.org/10.1016/j.compositesb.2012.11.006
3. Barbero, E.J., Raftoyiannis, I.G., 1994. Lateral and distortional buckling of pultruded I-beams. Composite Structures 27, 261–268. https://doi.org/10.1016/0263-8223(94)90087-6
4. Baylor, R.N., 2021. A Parametric Study of Lateral-Torsional Buckling in Pultruded FRP Beams Using Abaqus (MS). West Virginia University Libraries. https://doi.org/10.33915/etd.10216
5. Correia, J.R., Branco, F.A., Silva, N.M.F., Camotim, D., Silvestre, N., 2011. First-order, buckling and post-buckling behaviour of GFRP pultruded beams. Part 1: Experimental study. Computers & Structures, Civil-Comp 89, 2052–2064. https://doi.org/10.1016/j.compstruc.2011.07.005
6. Davalos, J.F., Qiao, P., 1997. Analytical and Experimental Study of Lateral and Distortional Buckling of FRP Wide-Flange Beams. Journal of Composites for Construction 1, 150–159. https://doi.org/10.1061/(ASCE)1090-0268(1997)1:4(150)
7. Estep, D.D., 2014. Bending and Shear Behavior of Pultruded Glass Fiber Reinforced Polymer Composite Beams With Closed and Open Sections - ProQuest. West Virginia, Morgantown,.
8. Ganesan, G., Kumaran, G., 2018. An experimental study on the behaviour of GFRP pultruded I beam reinforced with CFRP laminates. IJATEE 5, 232–242. https://doi.org/10.19101/IJATEE.2018.545012
9. Halim, A.H., 2020. Lateral torsional buckling of thin-walled rectangular and I-section laminated composite beams with arbitrary layups. KANSAS STATE UNIVERSITY, Manhattan, Kansas.
10. Karthick, K., Soundararajan, M., Kasiviswanathan, M., 2023. Torsional behavior of laminated composite FRP beams. AIP Conference Proceedings 2856, 040003. https://doi.org/10.1063/5.0165251
11. Liu, T., 2017. STABILITY BEHAVIOR OF PULTRUDED GLASS-FIBER REINFORCED POLYMER I-SECTIONS SUBJECT TO FLEXURE (PhD Thesis). University of Pittsburgh.
12. Liu, T., Harries, K.A., 2018. Flange local buckling of pultruded GFRP box beams. Composite Structures 189, 463–472. https://doi.org/10.1016/j.compstruct.2018.01.101
13. Liu, T., Vieira, J.D., Harries, K.A., 2019. Lateral torsional buckling and section distortion of pultruded GFRP I-sections subject to flexure. Composite Structures 225, 111151. https://doi.org/10.1016/j.compstruct.2019.111151
14. Mottram, J.T., 1992. Lateral-torsional buckling of a pultruded I-beam. Composites 23, 81–92. https://doi.org/10.1016/0010-4361(92)90108-7
15. Pandey, M.D., Kabir, M.Z., Sherbourne, A.N., 1995. Flexural-torsional stability of thin-walled composite I-section beams. Composites Engineering 5, 321–342. https://doi.org/10.1016/0961-9526(94)00101-E
16. Qiao, P., Zou, G., Davalos, J., 2002. EXPERIMENTAL AND ANALYTICAL EVALUATION OF LATERAL BUCKLING OF FRP COMPOSITE CANTILEVER I-BEAMS.
17. Sapkás, Á., Kollár, L.P., 2002. Lateral-torsional buckling of composite beams. International Journal of Solids and Structures 39, 2939–2963. https://doi.org/10.1016/S0020-7683(02)00236-6
18. Silva, N.M.F., Camotim, D., Silvestre, N., Correia, J.R., Branco, F.A., 2011. First-order, buckling and post-buckling behaviour of GFRP pultruded beams. Part 2: Numerical simulation. Computers & Structures, Civil-Comp 89, 2065–2078. https://doi.org/10.1016/j.compstruc.2011.07.006
19. Singh, S.B., Chawla, H., 2019. Stability and failure characterization of fiber reinforced pultruded beams with different stiffening elements, Part I: Experimental investigation. Thin-Walled Structures 141, 593–605. https://doi.org/10.1016/j.tws.2018.10.020
20. Thumrongvut, J., Seangatith, S., 2011. Experimental Study on Lateral-Torsional Buckling of PFRP Cantilevered Channel Beams. Procedia Engineering, The Proceedings of the Twelfth East Asia-Pacific Conference on Structural Engineering and Construction 14, 2438–2445. https://doi.org/10.1016/j.proeng.2011.07.306
21. Timoshenko, S.P., Gere, J.M., 2012. Theory of Elastic Stability. Courier Corporation.
22. Vieira, E.D.S., Vieira, J.D., Cardoso, D.C.T., 2018. LOCAL BUCKLING OF PULTRUDED GFRP I-SECTION SUBJECT TO BENDING, in: Proceedings of the 4th Brazilian Conference on Composite Materials. Presented at the Brazilian

Conference on Composite Materials, Pontifícia Universidade Católica do Rio de Janeiro, pp. 447–455. https://doi.org/10.21452/bccm4.2018.06.05
23. Vieira, J.D., Liu, T., Harries, K.A., 2018. Flexural stability of pultruded glass fibre-reinforced polymer I-sections. Proceedings of the Institution of Civil Engineers - Structures and Buildings 171, 855–866. https://doi.org/10.1680/jstbu.16.00238
24. Zeinali, E., Nazari, A., Showkati, H., 2024. Numerical Evaluation of Lateral Torsional Buckling of PFRP Channel Beams under Pure Bending. Sustainability 16, 303. https://doi.org/10.3390/su16010303

Arabic Abstract

صالح محمد العقلاء
كلية الهندسة
جامعة القصيم

تتناول هذه الدراسة تأثير اتجاه الألياف وتسلسل التكديس على سلوك عزوم الانبعاج والالتواء الجانبي (LTB) للعارضات المصنوعة من ألياف البلاستيك المقوى .(FRP) تم تقييم قدرة الانبعاج والالتواء الجانبي للعارضات باستخدام نموذج رقمي ثلاثي الأبعاد تم تصحيحه بناءا على التجارب، مما يسمح بتغيير تسلسل التكديس واتجاه الألياف. تم فحص عدة تسلسلات للتكديس من خلال تغيير زوايا الألياف. أظهرت العارضات ذات طبقات الألياف الأحادية الاتجاه مقاومة مثلى للانبعاج والإلتواء الجانبي عندما كانت ألياف الحافة لمقطع العارضة مصطفة على المحور الطولي (0°) وألياف الجزء الوسطي من العارضة مائلة بزاوية 45°. أدت الانحرافات عن هذه الزوايا إلى انخفاض كبير في قدرة الانبعاج والإلتواء الجانبي. أظهرت تسلسلات التكديس التي تضم مزيجاً من طبقات متقاطعة وطبقات مائلة أداءً أفضل في الانبعاج والالتواء الجانبي والعزمي مقارنةً بالتكوينات ذات الطبقات المائلة البحتة. بالإضافة إلى ذلك، تستكشف الدراسة تأثير اتجاه الألياف على السماكة المطلوبة للحافة لمقطع العارضة لتحقيق حمل معين في الانبعاج والالتواء الجانبي والعزمي. تشير النتائج إلى أن الزوايا الحادة الأقل في الحواف لمقطع العارضة (الفلانجة) تسمح بتصاميم حواف اقل سماكة. تؤكد هذه النتائج على أهمية تحسين اتجاه الألياف وتسلسل التكديس خلال تصميم عارضات FRP لتعظيم مقاومتها للانبعاج والالتواء الجانبي والعزمي وتحقيق قدرة تحميل فعالة.

كلمات مفتاحية: الانبعاج و الالتواء الجانبي، البوليمرات المقواة بالألياف، اتجاه الالياف، ترتيب طبقات رقائق البوليمر